

# A multi-scale model of the interplay between cell signalling and hormone transport in specifying the root meristem of *Arabidopsis thaliana*

D. Muraro<sup>a,b,\*</sup>, A. Larrieu<sup>a</sup>, M. Lucas<sup>a,c</sup>, J. Chopard<sup>d</sup>, H. Byrne<sup>a,e,f</sup>,  
C. Godin<sup>d</sup>, J. King<sup>a,f</sup>

<sup>a</sup>Centre for Plant Integrative Biology, University of Nottingham, Loughborough LE12 5RD, UK

<sup>b</sup>The Weatherall Institute of Molecular Medicine, University of Oxford, Oxford OX3 9DS, UK

<sup>c</sup>Equipe Rizogénese, UMR DIADE, IRD, 34394 Montpellier, France

<sup>d</sup>Virtual Plants Project-Team, UMR AGAP, INRIA/CIRAD, Montpellier, France

<sup>e</sup>Mathematical Institute, University of Oxford, Oxford, OX2 6GG, UK

<sup>f</sup>School of Mathematical Sciences, University of Nottingham, Nottingham NG7 2RD, UK

---

## Abstract

The growth of the root of *Arabidopsis thaliana* is sustained by the meristem, a region of cell proliferation and differentiation which is located in the root apex and generates cells which move shootwards, expanding rapidly to cause root growth. The balance between cell division and differentiation is maintained via a signalling network, primarily coordinated by the hormones auxin, cytokinin and gibberellin. Since these hormones interact at different levels of spatial organisation, we develop a multi-scale computational model which enables us to study the interplay between these signalling networks and cell-cell communication during the specification of the root meristem. We investigate the responses of our model to hormonal perturbations, validating the results of our simulations against experimental data. Our simulations suggest that one or more additional components are needed to explain the observed expression patterns of a regulator of cytokinin signalling, ARR1, in roots not producing gibberellin. By searching for novel network components, we identify two mutant lines that affect significantly both root length and meristem size, one of which also differ-

---

\*Corresponding author

Email address: Daniele.Muraro@ndm.ox.ac.uk (D. Muraro)

entially expresses a central component of the interaction network (SHY2). More generally, our study demonstrates how a multi-scale investigation can provide valuable insight into the spatio-temporal dynamics of signalling networks in biological tissues.

*Keywords:* gene networks, plant hormones, tissue differentiation

---

## 1. Introduction

*Arabidopsis thaliana* is a small annual weed that has been widely used in plant research as a model organism. Several features make this particular plant amenable to genetic and molecular studies. These include its small size (about 5 20 cm), relatively short generation time (8-10 weeks), high fecundity and small, compact genome [1]. The growth of the *Arabidopsis* root is sustained by the root apical meristem. This is a region of dividing cells near the tip of the root. Within this are four undifferentiated cells known as the quiescent centre (QC), which has properties analogous to a stem cell niche in animal systems (i.e. 10 slowly dividing, pluripotency). The QC is surrounded by differentiated cells that divide several times and form the rest of the meristem. After a number of divisions, cells have moved shootwards and enter the transition zone where they stop dividing and start elongating in the longitudinal direction. In order to maintain root stability, the specification of these tissues must be maintained 15 during growth. The plant hormone families auxin, cytokinin and gibberellin play key roles in controlling this developmental programme [2].

Upon seed germination, and at early stages of root development, increased cell proliferation causes the expansion of the root meristem until approximately 5 days post germination (5 dpG) [3]. This process is influenced by interactions 20 between several different signalling pathways and is coordinated by the plant hormone families auxin, cytokinin and gibberellin [2], [3].

Auxin (IAA) plays a central role in root development, regulating the positioning and formation of the meristem, and stimulating mitotic activity [4], [5]. Auxin is transported from the shoot to the root apex through cell membranes

25 by the combined action of influx and efflux transporters, named AUX/LAX and PIN proteins respectively. It then accumulates in the QC and columella cells whence it is redistributed shootwards (via the root cap and the epidermal cells), where it promotes cell proliferation [6], [7].

Cytokinin (CK) is antagonistic to auxin and regulates the activity of the  
30 meristem by negatively modulating auxin transport [8], [9]. Exogenous application of cytokinin, or over-expression of the IPT5 (Isopentenyltransferase 5) gene, which is responsible for cytokinin biosynthesis, reduces mitotic activity by promoting cell differentiation [10], [11].

Gibberellin (GA) is involved in several developmental processes in plants,  
35 including stem and leaf growth, seed germination and flowering time [12]. In roots, it is active primarily during the early stages of development, when it sustains auxin transport and promotes cell proliferation [3].

While cross-talk among these three hormone families is still poorly understood, a network scheme that integrates their signalling pathways has been  
40 proposed [3]. In this scheme, gibberellin levels act as a switch: high gibberellin levels antagonise cell differentiation during early growth (3 dp), whereas at about 5 dp, a decrease in gibberellin levels in the adult root reduces cell proliferation in the meristem.

Several mathematical models have been proposed to investigate the forma-  
45 tion of plant hormone gradients during root development in a multi-cellular framework [13], [14], [15], [16], [17] and their hormonal cross-talk at the single-cell level [18], [19]. However, the influence of the integrated cross-talk pathway between auxin, cytokinin and gibberellin on meristem development has not been modelled in root geometries derived from a segmented root image. The situ-  
50 ation is complicated by hormone fluxes between cells that influence, and are influenced by, the dynamics of the signalling network in each cell. As described above, auxin flux is the result of a multi-scale process which includes cross-talk between cytokinin and gibberellin. Moreover, a heterogeneous spatial distribution of auxin concentration has different effect on the biosynthesis of the  
55 other hormones leading, as a result, to different responses in their signalling

networks. Inclusion of these interactions in a multi-scale model permits analysis of the ways in which auxin flux may vary when other root hormones are perturbed and investigation of the time evolution of the network response in different root tissues. Finally, the results of our simulations can be qualitatively  
60 validated using confocal or reporter-based images. In this paper, we develop a multi-scale model of the cross-talk between auxin, cytokinin and gibberellin and use it to study their roles in the development of the meristem of Arabidopsis roots. We validate our simulations against confocal and reporter-based images of untreated roots. Additional model simulations of hormonal treatments reveal  
65 that one or more additional regulators are needed to inhibit the expression of the protein ARR1 in the meristem. By selecting, from a gene expression map, genes whose expression profiles are more highly expressed in this root region, we identify experimentally two mutants that affect meristem size. RT-qPCR data generated for these mutants show that one of them also affects the expression  
70 of SHY2, a key component of the signalling network, extending the network of known interactions.

## 2. Biological and modelling background

Control of root meristem size and root growth between 3 dpg and 5 dpg is influenced by the cross-talk between cytokinin and auxin [2], [3]; this occurs  
75 through signalling pathways converging on the SHY2 (SHORT HYPOCOTYL 2) gene, a member of the Aux/IAA gene family, which is part of the auxin response network [5] (see Figure 1). Moubayidin and co-workers showed that cell differentiation is promoted by high levels of the SHY2 protein [3]. SHY2 regulates meristem size by altering the balance between auxin and cytokinin  
80 signalling, the former acting as an inhibitor and the latter as a promoter of SHY2 levels. It achieves this effect by repressing some members of the PIN protein family, which are auxin efflux transporters, and (in so doing) slows down PIN-mediated auxin transport. SHY2 expression is promoted by cytokinin signalling as follows. Cytokinin binds reversibly to the AHK receptors, which auto-



85 phosphorylate, forming the complex Ck:AHKph. Subsequently, phosphorylated  
 AHKs phosphorylate AHPs inducing their translocation to the nucleus where  
 they phosphorylate in turn a family of transcription factors, the B-type ARRs  
 (mainly ARR1 and ARR12 in the root meristem). We model this process by  
 assuming that the complex Ck:AHKph transfers its phosphoryl group to ARR1  
 90 and ARR12 [2]. Both ARR1 and ARR12 promote SHY2 expression. ARR12  
 expression is not regulated by gibberellin, whereas ARR1 is down-regulated  
 by gibberellin, which promotes degradation of a member of the DELLA fam-  
 ily, namely RGA. The biosynthesis of auxin and gibberellin is also influenced  
 by other hormones, as follows. Cytokinin promotes auxin biosynthesis [20],  
 95 auxin up-regulates the expression of genes involved in gibberellin metabolism  
 [21] while suppressing cytokinin biosynthesis [22]. At early stages of growth (3  
 dpd), high levels of gibberellin selectively repress ARR1 and, as a result, cell  
 division dominates cell differentiation. At 5 dpd, the meristem reaches maturity  
 and a decrease in the rate of gibberellin biosynthesis relieves the repression of  
 100 ARR1, leading to a decrease in the rate of cell proliferation [3].

We have developed a multi-scale model, based on differential equations, to in-  
 vestigate the interactions among the signalling pathways associated with auxin,  
 cytokinin and gibberellin in a longitudinal root section. The model embeds the  
 signalling pathways described above in every cell of a multicellular geometry de-  
 105 rived from a segmented root image. As we will show in the Results section, our  
 model contains an unknown component which acts as a repressor of ARR1. In  
 what follows we will denote this subcellular component X. A schematic diagram  
 of this network and of the representative root tissue are presented in Figure 1.  
 The species and the reactions incorporated in our model include those proposed  
 110 by Moubayidin et al. [3], accounting for phosphorylation and for regulation of  
 hormonal biosynthesis. The reactions that constitute our signalling network are  
 listed in the Supplementary Material. From this set of reactions we derive a sys-  
 tem of ordinary differential equations governing the dynamics of the interaction  
 network. The computational tools used to simulate our model are described in  
 115 the Materials and Methods section, whereas a detailed description of the model

reactions and equations, together with the results of a parameter sensitivity analysis, is reported in the Supplementary Material.

Based on previous single-cell models [15], [19], [23] we model regulation of mRNA levels in a particular cell using Michaelis-Menten kinetics. Auxin transport is modelled using a modified version of the Flux based polarization model developed by Stoma et al. [24] (see equations (1) and (2) below), where we specify, as part of the root template, the sides of the cell on which PIN proteins are present. The boundary conditions applied to the cells at the most shootwards end of the spatial domain are that auxin concentration is constant for the vasculature cells, and that there is zero efflux (in a shootwards direction) from the other cells. For simplicity, we follow [13] in ignoring the contribution of auxin influx transporters.

In Arabidopsis, the PIN family consists of eight members [25]. In our model, we group this family into a single, representative protein whose spatial distribution is consistent with PIN expression data from confocal images and the multi-cellular model proposed in [13]. Since the network controlling the size of the meristem is known to act on the PIN proteins located in the vascular tissues (PIN1, 3, 7), we assume that only the PINs in this tissue are transcriptionally repressed by SHY2, and we assign constant PIN transcription in the external layers. In particular, PIN1, 3, 7 are expressed in the vascular tissue and PIN3 is also expressed in the columella; we also account for SHY2 in the columella as it appears to be weakly expressed in this region both at 3 dpv and at 5 dpv in untreated roots and in roots grown 4 hr on 5 mM transzeatin (Zt) (see Figures 1 a,b,g,h in Moubayidin et al. [3]). Low levels of SHY2::GUS were also detected in the columella by Scacchi et al. (Figure 2A [26]). Within each cell, PIN proteins are distributed on those cell walls where the proteins are known to be present (see Supplementary Figure 1).

The concentrations of PIN proteins at these specified membrane domains vary depending on the flux of auxin through the cell walls. Between two neighbouring cells, the flux due to passive auxin diffusion follows a discrete form of Fick's First Law, whereas active auxin transport depends on the efficiency of

PIN transporters [27]. More precisely, denoting by  $[\text{Aux}]_i$  the concentration of auxin in cell  $i$ ,  $V_i$  the cell size,  $N_i$  the set of cells neighbouring cell  $i$  and  $S_{i,n}$  the cell wall between cells  $i$  and  $n$ , we assume that the auxin concentration in cell  $i$  is governed by the equation

$$\frac{d[\text{Aux}]_i}{dt} = -\frac{1}{V_i} \sum_{n \in N_i} S_{i,n} (J_{i \rightarrow n}^P + J_{i \rightarrow n}^T) + p_{\text{Aux}} F_{\text{Aux}}^{(i)} - d_{\text{Aux}} [\text{Aux}]_i, \quad (1)$$

where  $p_{\text{Aux}}$ ,  $d_{\text{Aux}}$  denote the production and degradation rate of auxin,  $J_{i \rightarrow n}^P = P_{\text{Aux}}([\text{Aux}]_i - [\text{Aux}]_n)$  is the flux of auxin due to passive transport and  $P_{\text{Aux}}$  represents the permeability of the cell wall;  $J_{i \rightarrow n}^T = T_{\text{Aux}}([\text{Aux}]_i [\text{PIN}_p]_{i,n} - [\text{Aux}]_n [\text{PIN}_p]_{n,i})$  is the flux of auxin due to active transport by PIN proteins of concentration  $[\text{PIN}_p]_{i,n}$  on  $S_{i,n}$  and  $T_{\text{Aux}}$  is the rate of active flux;  $F_{\text{Aux}}^{(i)}$  is a functional form controlling auxin biosynthesis given by

$$F_{\text{Aux}}^{(i)} = b_{\text{Aux}} + \frac{([\text{Ck}]_i / \theta_{\text{Ck}})}{1 + ([\text{Ck}]_i / \theta_{\text{Ck}})} \quad (2)$$

where  $b_{\text{Aux}}$  is a parameter regulating basal auxin production in all tissues and  $\theta_{\text{Ck}}$  is the cytokinin binding threshold. Cytokinin and gibberellin fluxes are  
145 governed by equations similar to those for auxin, except that active transport is neglected and zero flux boundary conditions are imposed on the cells on the boundary of the computational domain.

Auxin controls cytokinin bio-synthesis [22], interacting with IPT5 and IPT7 [28], and most auxin-resistant mutants also show changes in their cytokinin sensitivity [29], [30]. The regions of biosynthesis of the cytokinin biosynthesis gene  
150 IPT5 (ATP/ADP-isopentenyltransferase 5) are localised in the vasculature at the elongation zone and in the root apex [2], whereas AtIPT7::GFP fluorescence was observed in the vascular stele of the elongation area [31]. Transcriptional and reporter analyses suggest that gibberellin biosynthesis occurs  
155 predominantly in the meristem [32], [33]. We model this by assuming tissue specific self-activation of gibberellin biosynthesis (see Supplementary Material).

As in most models of signalling networks based on differential equations, the predicted qualitative outcome of the model is dependent on the choice of the parameter values (e.g. production and degradation rates, protein-DNA binding

thresholds), many of which are unknown [18], [34]. Following [18], [35], we have  
 based our estimates of the ratio between the rates of auxin transport and per-  
 meability on those used in previous models [13], [35], [36], whereas other values  
 have been chosen manually to ensure agreement with patterns experimentally  
 observed. In order to determine the degree to which parameter variation affects  
 the outcome of our model of hormonal cross-talk we have performed a global  
 parameter sensitivity analysis at a single-cell level in all root regions in which  
 the parameters have different, tissue specific values. In this way, we identified  
 those parameters to which the model is most sensitive, these being mainly asso-  
 ciated with gibberellin, RGA and auxin regulation. Guided by the results of this  
 single-cell analysis, we used the multi-cellular model to perform a multi-cellular  
 local sensitivity analysis with respect to these parameters, together with those  
 associated with transport and permeability. Since SHY2 is regulated negatively  
 by auxin and positively by the cytokinin pathway, we also used the multi-cellular  
 model to study sensitivity to parameters associated with such regulation. The  
 parameters identified by the single-cell sensitivity analysis mainly affect gib-  
 berellin, RGA, ARR1, SHY2 and Ck:AHK; the parameters associated with  
 transport and permeability mainly influence auxin, cytokinin, phosphorylated  
 ARR12 and gibberellin; the parameters associated with SHY2 regulation mainly  
 influence SHY2, auxin, cytokinin. We also investigated whether tissue-specific  
 permeability rates ( $P_{Aux}$ ,  $P_{CK}$ ,  $P_{GA}$ , see Supplementary Material) may affect  
 the formation of the simulated protein patterns. To this end, we extended our  
 sensitivity analysis by randomly varying the values of  $P_{Aux}$ ,  $P_{CK}$ ,  $P_{GA}$  in dif-  
 ferent cell types up to two-fold in comparison to default values. These changes  
 did not significantly affect the simulation results. The patterns obtained when  
 varying these parameters, considering as default the parameter values used to  
 simulate an untreated root (Supplementary Movie 5), are reported in the Sup-  
 plementary File ‘Permeability\_Sensitivity.pdf’.

A detailed description of this analysis is reported in the Supplementary Ma-  
 terial.



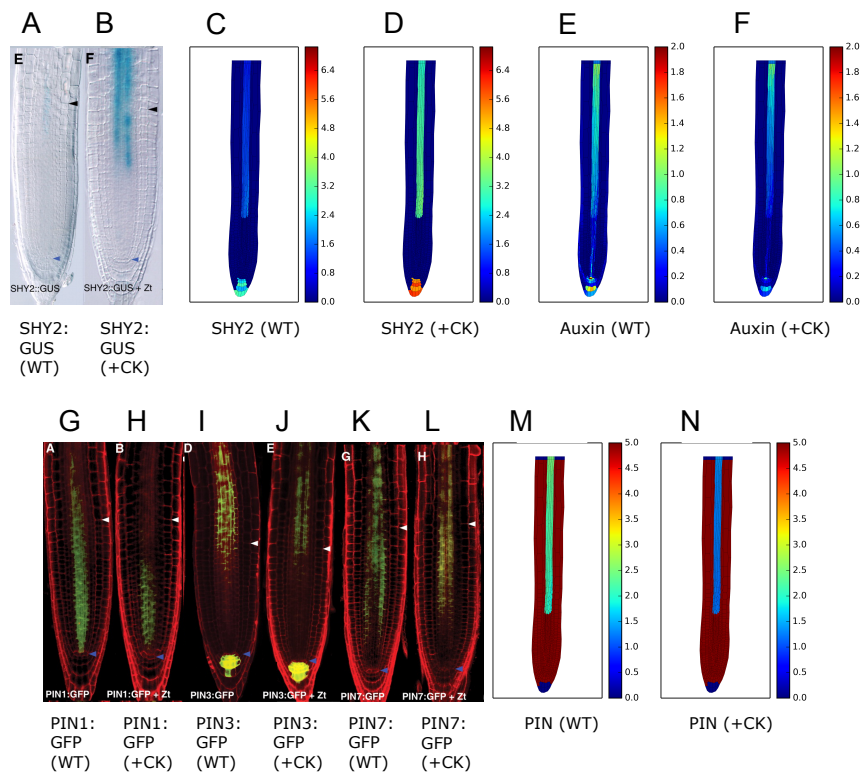
Supplementary Movie 1 and Moubayidin et al. [3]). The inhibitory role of gibberellin means that RGA reaches higher concentration levels in the elongation zone; consequently, ARR1 mimics the higher expression of its activator RGA in the elongation zone (see Supplementary Movie 1). Our model enables us to predict the spatial distributions and dynamics of auxin, cytokinin and gibberellin, providing a visualisation of hormones whose concentrations cannot be easily measured experimentally but which affect other measurable network components. In particular, auxin is actively transported through the vasculature from the basal tissues to the root cap where it is re-directed towards the stele through the external root layers (see Supplementary Movie 1). These auxin dynamics are consistent with those generated from other multi-cellular models of auxin transport, such as [13], that do not include a subcellular interaction network. Guided by our simulations of the untreated root, we now apply hormonal perturbations to our computational model and compare the results with confocal and staining images obtained from experiments performed under similar conditions.

### 3.2. Model predictions for roots grown on transzeatin

The number of cells in the root meristem shows an average decrease under treatment for 12 hours with  $5\mu M$  of a member of the cytokinin family (transzeatin, Zt) [10]. We now investigate how an increase in the rate of biosynthesis of cytokinin may affect the patterns observed in untreated roots (see Figure 2 and Supplementary Movie 2a). Figure 2B reveals that SHY2 expression at 5 dpg is clearly visible in the vasculature of the elongation zone and is more strongly induced by the higher cytokinin levels. This induction reduces the size of the region in which PINs are expressed in cytokinin-treated roots, prompting greater cell differentiation (see Figures 2G-L) [10]. In our computational simulations, over-production of cytokinin in its biosynthesis regions leads to an increase in the phosphorylation of ARR1 and ARR12. The higher levels of active ARRs (ARR1ph, ARR12ph) promote SHY2 expression in the region of cytokinin biosynthesis (see Figure 2D and Supplementary Movie 2a). SHY2

represses PIN genes in the vasculature and causes down-regulation of PIN expression in the elongation zone (see Figure 2N and Supplementary Movie 2a).

We also use our model to predict how the flux of auxin may be affected by cytokinin over-expression and the subsequent degradation of PIN proteins in the vascular tissue. In our simulations, the greater the abundance of the PINs, the higher the flux of auxin; consequently, the degradation of PIN proteins, caused by cytokinin over-expression, hinders the transport of auxin, which tends to accumulate where PIN levels are low, namely in the elongation zone (see Figure 2F). Simulating the same treatment by varying where the basal boundary of the meristem is defined did not show qualitative differences in the expression pattern (see Supplementary Movie 2b).



---

Figure 2 (*previous page*): **Untreated roots and roots grown on transzeatin.** A-B) SHY2::GUS expression in root meristems at 5 dpd of untreated roots (A) and of roots grown on 5  $\mu M$  transzeatin (Zt), (B). C-D) SHY2 protein expression in our multi-scale model in untreated roots (C) and in roots with higher cytokinin biosynthesis rate (D); cytokinin activates SHY2 transcription via the phosphorylation of ARR1 and ARR12, enhancing SHY2 protein levels in the vasculature at the elongation zone. E-F) Simulated auxin flow in untreated roots (E) and in roots with higher cytokinin biosynthesis rate (F). Auxin flows from the apical vasculature to the root cap, part of auxin then being redirected towards the shoot via the epidermal cells. When cytokinin is over-expressed, the flux is hindered by the degradation of PIN proteins and auxin tends to accumulate into regions of low PIN activity, namely the elongation zone. G-L) PIN1,3,7::GFP expression in root meristems of untreated roots at 5 dpd (G,I,K) and in cytokinin treated roots (5  $\mu M$  Zt), (H,J,L). M-N) PIN protein expression in our multi-scale model in untreated roots (M) and in roots with higher cytokinin biosynthesis rate (N); the higher activity of SHY2 down-regulates PIN expression in the vascular tissue. A detailed description of the equations and parameters used in our simulations is reported in the Supplementary Material. In Figures A-B) and G-L) blue and white arrowheads indicate the quiescent centre and the beginning of the cortex elongation zone, respectively; these figures are reproduced with permission from [3], [10]. (For interpretation of the references to colour in this figure caption, the reader is referred to the web version of this article).

### 3.3. The joint action of auxin and gibberellin reproduces the observed distribution of RGA

Since RGA levels are low where the concentration of gibberellin is high, the RGA:GFP reporter can be used to estimate the levels and spatial distribution of gibberellin. When Moubayidin et al. [3] analysed confocal images to determine the average pixel intensity of the RGA:GFP reporter at 3 and 5 dpd they found RGA:GFP fluorescence to be significantly higher at 5 dpd than at 3 dpd, but not uniform in all root tissues, being concentrated in the elongation zone and the cortex (see Supplementary Figure S2I [3]). RGA expression depends on gibberellin biosynthesis which, in turn, is promoted by auxin [21]. In our model, most of the auxin flux is through the vascular tissue, so auxin accumulates in the columella and in the QC. Subsequently, some auxin flows back via the epidermis. We assume that the combination of the self- and auxin-mediated activation of gibberellin determines the spatial distribution of RGA. At 3 dpd



gibberellin is present at higher concentrations [3]. For this reason, we suppose that the network response of the untreated root at 3 dpv is analogous to the network response of a root over-producing gibberellins and we compare simulations having gibberellin biosynthesis higher than that in an untreated root with confocal and staining images of roots at 3 dpv. The simulation results are shown in Figures 3C, 3D and in Supplementary Movie 3a. At 3 dpv, the concentration of RGA is uniformly low because of the over-production of gibberellin (see Figures 3A, 3C and Supplementary Movie 3a), whereas at 5 dpv the heterogeneous distribution of gibberellin in the root tissues causes the concentration of RGA to peak in the cortex (see Figures 3B, 3D and Supplementary Movie 1). Simulating gibberellin over-expression by varying where the basal boundary of the meristem is defined did not lead to qualitative differences in the expression pattern (see Supplementary Movies 3a, 3b).

### 3.4. *Roots grown on gibberellin and PAC*

ARR1:GUS expression in untreated roots is localised in the elongation zone (see Figure 3E). Its expression is not detectable when the root is grown on gibberellin (see Figure 3F), whereas it is enhanced when gibberellin levels are reduced using a pharmacological approach (PAC treatment; see Figure 3G). While our simulations under gibberellin treatment (Supplementary Movies 3a, 3b) yield lower levels of ARR1 expression than those of untreated roots (Supplementary Movie 1), and these lower levels could not be detectable with the ARR1:GUS reporter (as shown in Figure 3F), regulation via RGA alone cannot explain the spatial distribution of ARR1 in PAC treated roots: the depletion of gibberellin biosynthesis would cause both RGA and ARR1 to be distributed approximately uniformly throughout the root (see Supplementary Movie 4), at higher levels than in an untreated root (see Supplementary Movie 1). This result is incompatible with the staining image of ARR1 for roots grown on PAC, which shows that its expression is lower in the meristem than in the elongation zone. In order to reproduce the observed expression pattern, we assume the existence of an extra regulator (or regulators) whose (combined) effect is to

285 repress ARR1 in the meristem, via either direct control of its transcription or  
down-regulation of RGA in the meristem. When this regulator (denoted by the  
letter X in Figure 1 and equations (1)-(4) in the Supplementary Material) is  
included, our model reproduces the experimentally observed patterns of ARR1  
under all treatments without influencing substantially the patterns of the other  
290 network components (see Figures 3H, 3I, 3J and Supplementary Movies 5-8).  
Similar simulation results are obtained if we assume direct repression of ARR1  
by X or indirect repression via RGA (see Supplementary Movie 9).

Independently of the inclusion of X, our model also predicts lower levels of  
ARR1 in the vascular tissue in the simulation of the untreated root at 5 dpg  
295 (see Figure 3H). These lower levels of ARR1 in the vasculature are due to RGA-  
mediated activation of ARR1 and may depend either on another regulatory  
mechanism not included in the model or on technical limitations of staining  
images that show ARR1 expression in external tissues.

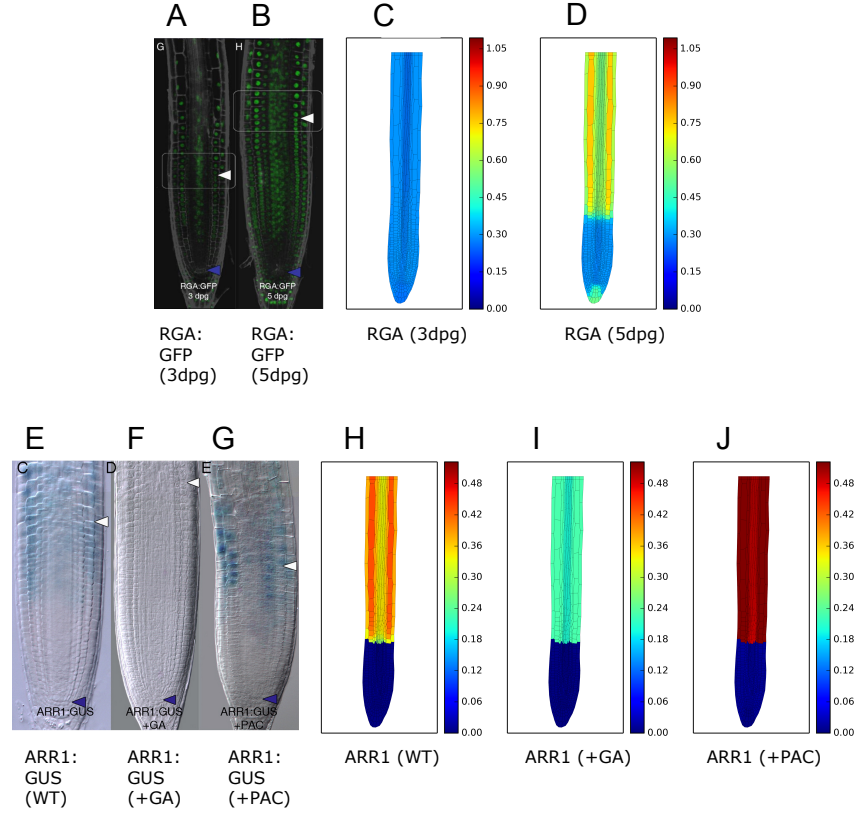


**Figure 3: Untreated roots, roots grown on gibberellin and roots grown on PAC.** A-B) RGA:GFP expression in root meristems at 3 dpv (A) and at 5 dpv (B). C-D) RGA protein expression in our multi-scale model in roots with higher gibberellin biosynthesis rate (C) and in untreated roots (D); RGA activity in the elongation zone increases at later stages of root meristem development due to the lower levels of gibberellin. E-G) ARR1:GUS expression in root meristems at 5 dpv of untreated roots (E), roots grown on 10  $\mu M$  gibberellin (F), and roots grown on 10  $\mu M$  paclobutrazol (PAC) (G). H-J) ARR1 protein expression in our multi-scale model in untreated roots (H), roots with gibberellin over-expressed (I), roots with simulated PAC treatment (J); gibberellin exerts an inhibitory effect on ARR1 activity. A detailed description of the equations and parameters used in our simulations is reported in the Supplementary Material. In Figures A-B) and E-G) blue and white arrowheads indicate the quiescent centre and the beginning of the cortex elongation zone, respectively; these figures are reproduced with permission from [3]. (For interpretation of the references to colour in this figure caption, the reader is referred to the web version of this article).

### 3.5. Novel components regulate root and meristem size

300 Based on our simulation results, we selected 77 genes from a gene expression map [37] whose expression profiles were most anti-correlated with *ARR1* and, as a consequence, were more highly expressed in the meristem. We then identified at least one homozygous T-DNA insertion line within the coding sequence of 34 of these 77 genes [38]. Comparison of the root lengths of the mutants with  
305 those of the WT led to the identification of 12 genes with a significantly different phenotype. Lines whose phenotype was confirmed in two subsequent generations were further selected.

This last selection led to the identification of three lines, which have mutations in the following three genes: an ELMO/CED-12 family protein (AT3G60260, that we term *aag1-1* for ARR1 anticorrelated gene 1), the CID3 ctc-interacting  
310 domain 3 protein (AT1G54170, *aag2-1*) and a transcription factor (AT1G68920, *aag3-1*). *aag1-1* and *aag3-1* mutants developed longer roots, whereas *aag2-1* developed shorter ones (see Figure 4). Consistently, meristem length was shorter for *aag2-1* and longer for *aag3-1* (results were not significant for *aag1-1*). In  
315 order to test whether the expression of several regulators of meristem length was affected in the mutants, their expression in roots tips was analysed using RT-qPCR. In *aag1-1* mutants several network components were down-regulated (*ARR1*, *ARR10* and *SHY2*). In *aag2-1* mutants only *SHY2* was affected while no network components showed differential expression in *aag3-1* mutants com-  
320 pared to the WT. These results suggest that compensatory mechanisms not included in the pathways analysed are also responsible for the absence of effects of other mutants on *ARR1* expression. Since our selection of mutants was not able to identify a gene playing the role of regulator X, we have analysed two further model setups. We investigated whether PAC treatment could specifically  
325 increase RGA levels in the elongation zone; however, simulation results showed that *ARR1* is still expressed in the meristem, although at lower levels than in the elongation zone (see Supplementary Movie 10). We also instead assumed that *ARR1* transcription is restricted to the elongation zone because RGA activation requires an X transcription factor which is expressed only in this area;

330 under this hypothesis our simulation shows that ARR1 is nearly absent in the meristem (see Supplementary Movie 11). Taken together, these results suggest lines of further research.

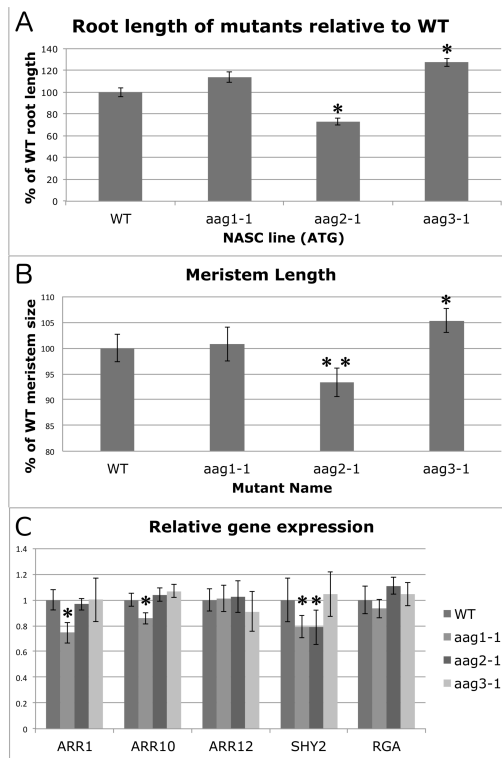


Figure 4: **Novel components regulating root and meristem size.** A) Root length of mutants relative to untreated roots. *aag1-1* and *aag3-1* mutants developed longer roots, whereas *aag2-1* developed shorter roots compared with untreated roots; however, only difference in root length in *aag2-1*, *aag3-1* is statistically significant (p-values  $< 10^{-4}$ ). B) Meristem size of mutants relative to untreated roots. *aag2-1* mutants developed shorter meristems (p-value  $< 0.05$ ), whereas *aag3-1* developed longer meristems compared with untreated roots (p-value  $\approx 0.07$ ). C) Relative expression levels of several genes involved in meristem size in *aag1-1*, *aag2-1* and *aag3-1* mutants compared with untreated roots. ARR1, ARR10 and SHY2 are expressed to lower levels in *aag1-1* mutants (p-values  $< 0.03$ ), whereas only SHY2 expression is affected in *aag2-1* (p-value  $< 0.05$ ). None of these genes are significantly affected in *aag3-1*. Single asterisks indicate statistical significance with p-value  $< 0.1$ , whereas the double asterisk indicates a p-value  $< 0.05$ .

## 4. Discussion

The organisation of the root meristem in *Arabidopsis* is established in the first five days following germination. During this time period, hormonal cross-talk regulates the balance between cell proliferation, differentiation and elongation. The regulation of these patterning events in the root apex involves complex interactions between three classes of signalling molecules, namely auxin, cytokinin and gibberellin [3]. Such interactions involve cross-talk at the subcellular and tissue scales, the former being mediated via a signalling network and the latter via auxin transport in different tissues which then influences levels of other network components.

When studying such systems, mathematical modelling can be used to perform *in silico* experiments designed to determine whether the current state of knowledge of the system is sufficient to explain the experimental data. It also permits visualisation of how the dynamics of hormonal signalling may change in response to specific perturbations, such visualisation not being easy to perform *in vivo*.

In this paper, we proposed a multi-scale computational model to investigate the specification of the root apical meristem in *Arabidopsis thaliana*. Although mathematical models have previously been used to analyse auxin transport in multi-cellular frameworks [13], [24], to our knowledge the cross-talk between auxin, cytokinin and gibberellin has not previously been modelled in a multi-cellular geometry. Our model accounts for two different levels of regulation: active and passive (diffusive) transport of hormones between cells and molecular interactions at the subcellular scale. Our model can reproduce the gene expression patterns observed experimentally in untreated roots and in those grown on transzeatin. The model simulations suggest that the signalling network proposed in [3] may not be sufficient to explain the spatial distributions of all of its components in roots grown on PAC. In particular, a regulator of cytokinin signalling (ARR1) has a specific expression pattern that we could not reproduce when performing model simulations. To account for this difference,

we introduced an additional inhibitor of ARR1 in our model and showed that it yields expression patterns similar to those observed *in vivo*.

365 In order to provide biological support for this model prediction we looked for candidate genes that could fulfil this function. Using published microarray datasets, we identified those genes whose expression profiles are most strongly anti-correlated with ARR1 in the root apical meristem. Of these mutants 3 lines (*aag1-1*, *aag2-1*, *aag3-1*) had root sizes that were either longer (*aag1-1* and *aag3-1*) or shorter (*aag2-1*) than their WT counterparts. RT-qPCR data generated 370 for these lines showed that *aag1-1* and *aag2-1* mutants express lower levels of SHY2. The *aag1-1* mutant also has a reduced expression of ARR1 and ARR10, suggesting an indirect regulation of SHY2 expression through ARR1. None of the mutated genes acts as a repressor of ARR1 in the manner required for the unknown component X, suggesting either that this component is not part of the 375 selected genes or that its role might be played by the combined action of distinct genes. Moreover, the effects of such genes on the phenotype suggests that other signalling pathways may affect the definition of the meristematic region. In addition, the influence of two of these mutations (*aag1-1* and *aag2-1*) on the expression levels of other components that control meristem size (SHY2 and 380 ARR1) suggests that these genes may act either directly, or indirectly via *ARR1*, as activators of *SHY2*, thereby extending the network of known interactions.

We conclude that computational modelling of the type performed here can serve as a valuable tool for predicting how specific perturbations affect the 385 spatio-temporal dynamics of the *Arabidopsis* root, yielding results that may not easily be visualised in the laboratory, and for determining when additional components are needed to interpret experimental data. Since the hormone concentration in each cell depends both on regulation of active transport by PIN proteins and single-cellular hormonal cross-talk, analysis of such dynamics requires a multi-scale approach. By selecting a biological hypothesis and interpreting 390 our simulation results, we identified candidate genes that may play an important role in determining root and meristem size. Our findings also highlight the potential benefits of interdisciplinary research. It provides a coherent

theoretical framework for testing whether the current understanding of how a  
395 system functions is compatible with observed behaviours and for identifying  
where additional experimental investigation is needed. Our analysis may stimu-  
late further investigation, from the experimental side, to analyse in more detail  
the spatio-temporal influence of the identified mutants on the other network  
components and, from the theoretical side, to extend the modelling framework  
400 to include further components of cell signalling and cell-to-cell communication,  
and into more realistic three-dimensional geometries.

## 5. Materials and Methods

### 5.1. Computational tools

The tissue representation is extracted from the OpenAlea framework [39].  
405 OpenAlea is an open source software project for Plant Architecture modelling.  
Libraries and tools are primarily based on the high level, object-oriented script  
language, Python. Cell wall geometry and PIN distribution are manually repro-  
duced from the experimental data of a root tissue using the open source software  
Inkscape [40]. A section of the root geometry is represented in Supplementary  
410 Figure 1. A detailed description of the reactions included in our model, the  
equations and associated parameters is presented in the Supplementary Mate-  
rial, together with the parameter sensitivity analysis.

### 5.2. Mutant lines

Homozygous SALK lines for the ARR1 anti correlated genes were ordered  
415 from the Nottingham Arabidopsis Stock Centre (NASC). The mutant lines with  
the original stock numbers are reported in the Supplementary Workbook.

### 5.3. Seed sterilisation, seedling growth and root length measurements

Seeds were surface sterilized for 5 minutes in 50% bleach, 0.1% triton X-  
100, and then washed three times with sterile ddH<sub>2</sub>O. Seeds were stratified at  
420 4°C for 2 days to synchronise germination. Root length was determined using



images of WT and mutant seedlings taken 7 days post germination with a Canon PowerShot G10 camera and analysed using Fiji (Fiji Is Just ImageJ) (<http://fiji.sc/Fiji>) (ImageJ version 1.41b) and Microsoft Excel 2007 (Microsoft Corporation, Redmond, USA).

#### 425 5.4. RNA extraction and RT-qPCR

RNA was extracted from plant tissues using Trizol Reagent (Invitrogen) and cleaned up using the RNeasy kit (Qiagen). Poly(dT) cDNA was prepared from 0.5 $\mu$ g total RNA with Superscript II reverse transcriptase (Invitrogen) and analyzed on a LightCycler 480 apparatus (Roche Diagnostics) with the Quantace SYBRGREEN mix (Quantace) according to the manufacturers' instructions. 430 Targets were quantified with specific primer pairs designed with the Universal Probe Library Assay Design Center (Roche Applied Science). All individual reactions were done in quadruplicate and data were statistically analyzed with Microsoft Excel 2007 (Microsoft Corporation, Redmond, USA). Expression levels 435 were normalized to At1G04850. The primer sequences that were used for the genotyping and RT-qPCR are reported in the Supplementary Workbook.

### Acknowledgments

We gratefully acknowledge the Biotechnology and Biological Research Council and the Engineering and Sciences Research Council for financial support as 440 part of the CISB programme award to CPIB. J.R. King gratefully acknowledges the funding of the Royal Society and Wolfson Foundation. The authors thank S. Úbeda-Tomás, L. Band, M. Bennett and J. Fozard for their support and feedback in the development this work.

### References

- 445 [1] Page DR, Grossniklaus U. 2002 The art and design of genetic screens: *Arabidopsis thaliana*. *Nat. Rev. Genetics* 3, 124-136.

- [2] Moubayidin L, Di Mambro R, Sabatini S. 2009 Cytokinin-auxin crosstalk. *Trends Plant Sci.* 14(10):557-62.
- [3] Moubayidin L, Perilli S, Dello Ioio R, Di Mambro R, Costantino P, Sabatini S. 2010 The rate of cell differentiation controls the Arabidopsis root meristem growth phase. *Curr. Biol.* 20, 1138-1143.
- [4] Blilou I, Xu J, Wildwater M, Willemsen V, Paponov I, Friml J, Heidstra R, Aida M, Palme K, Scheres B. 2005 The PIN auxin efflux facilitator controls growth and patterning in Arabidopsis roots. *Nature* 433:39-44.
- [5] Dello Ioio R, Linhares FS, Scacchi E, Casamitjana-Martinez E, Heidstra R, Costantino P, Sabatini S. 2007 Cytokinins determine Arabidopsis root-meristem size by controlling cell differentiation. *Curr. Biol.* 17:678-682.
- [6] Kramer EM, Bennett MJ. 2006 Auxin transport: a field in flux. *Trends Plant Sci.* 11:382-386.
- [7] Perrot-Rechenmann C. 2010 Cellular responses to auxin: division versus expansion. *Cold Spring Harb. Perspect. Biol.* 2(5):a001446.
- [8] Ruzicka K, Simásková M, Duclercq J, Petrášek J, Zazimalová E, Simon S, Friml J, Van Montagu MC, Benková E. 2009 Cytokinin regulates root meristem activity via modulation of the polar auxin transport. *Proc. Natl. Acad. Sci. U. S. A.* 106(11):4284-9.
- [9] Marhavý P, Bielach A, Abas L, Abuzeineh A, Duclercq J, Tanaka H, Pařezová M, Petrášek J, Friml J, Kleine-Vehn J, et al. 2011 Cytokinin modulates endocytic trafficking of PIN1 auxin efflux carrier to control plant organogenesis. *Dev. Cell.* 21(4):796-804.
- [10] Dello Ioio R, Nakamura K, Moubayidin L, Perilli S, Taniguchi M, Morita MT, Aoyama T, Costantino P, Sabatini S. 2008 A genetic framework for the control of cell division and differentiation in the root meristem. *Science* 322(5906):1380-4.

- [11] Chavarria-Krauser A, Schurr U. 2004 A cellular growth model for root tips.  
475 *J. Theor. Biol.* 230(1):21-32.
- [12] Sun TP, Gubler F. 2004 Molecular mechanism of gibberellin signaling in  
plants. *Annu. Rev. Plant Biol.* 55:197-223.
- [13] Grieneisen VA, Xu J, Marée AF, Hogeweg P, Scheres B. 2007 Auxin trans-  
port is sufficient to generate a maximum and gradient guiding root growth.  
480 *Nature* 449(7165):1008-13.
- [14] Band LR, Wells DM, Larrieu A, Sun J, Middleton AM, French AP, Brunoud  
G, Sato EM, Wilson MH, Péret B, et al. 2012 Root gravitropism is reg-  
ulated by a transient lateral auxin gradient controlled by a tipping-point  
mechanism. *Proc. Natl. Acad. Sci. U. S. A.* 109(12):4668-73.
- 485 [15] Muraro D, Byrne H, King J, Bennett M. (2013) The role of auxin and  
cytokinin signalling in specifying the root architecture of *Arabidopsis*  
*thaliana*. *J. Theor. Biol.* 317:71-86.
- [16] Band LR, Wells DM, Fozard JA, Ghetiu T, French AP, Pound MP, Wilson  
MH, Yu L, Li W, Hijazi HI, et al. 2014 Systems analysis of auxin transport  
490 in the *Arabidopsis* root apex. *Plant Cell* 26(3):862-75.
- [17] Cruz-Ramírez A, Díaz-Triviño S, Blilou I, Grieneisen VA, Sozzani R, Za-  
mioudis C, Miskolczi P, Nieuwland J, Benjamins R, Dhonukshe P, et al.  
2012 A bistable circuit involving SCARECROW-RETINOBLASTOMA in-  
tegrates cues to inform asymmetric stem cell division. *Cell* 150(5):1002-15.
- 495 [18] Liu J, Mehdi S, Topping J, Tarkowski P, Lindsey K. 2010 Modelling and  
experimental analysis of hormonal crosstalk in *Arabidopsis*. *Mol. Syst. Biol.*  
6:373.
- [19] Muraro D, Byrne H, King J, Voss U, Kieber J, Bennett M. 2011 The  
influence of cytokinin-auxin cross-regulation on cell-fate determination in  
500 *Arabidopsis thaliana* root development. *J. Theor. Biol.* 283(1):152-67.

- [20] Jones B, Gunnerås SA, Petersson SV, Tarkowski P, Graham N, May S, Dolezal K, Sandberg G, Ljung K. 2010 Cytokinin regulation of auxin synthesis in Arabidopsis involves a homeostatic feedback loop regulated via auxin and cytokinin signal transduction. *Plant Cell* 22, 9, 2956-2969.
- 505 [21] Frigerio M, Alabadí D, Pérez-Gómez J, García-Cárcel L, Phillips AL, Hedden P, Blázquez MA. (2006) Transcriptional regulation of gibberellin metabolism genes by auxin signaling in Arabidopsis. *Plant Physiol.* 142:553-563.
- [22] Nordström A, Tarkowski P, Tarkowska D, Norbaek R, Astot C, Dolezal  
510 K, Sandberg G. Auxin regulation of cytokinin biosynthesis in Arabidopsis thaliana: a factor of potential importance for auxin-cytokinin-regulated development. *Proc. Natl. Acad. Sci. U S A.* 2004 May 25;101(21):8039-44. Epub 2004 May 14.
- [23] Rice JJ, Tu Y, Stolovitzky G. 2005 Reconstructing biological networks  
515 using conditional correlation analysis. *Bioinformatics* 21(6):765-73.
- [24] Stoma S, Lucas M, Chopard J, Schaedel M, Traas J, Godin C. 2008 Flux-based transport enhancement as a plausible unifying mechanism for auxin transport in meristem development. *PLoS Comput. Biol.* 4(10):e1000207.
- [25] Zazimalová E, Murphy AS, Yang H, Hoyerová K, Hosek P. 2010 Auxin  
520 transporters - Why so many? *Cold Spring Harb. Perspect. Biol.* 2(3):a001552.
- [26] Scacchi E, Salinas P, Gujas B, Santuari L, Krogan N, Ragni L, Berleth T, Hardtke CS. 2010 Spatio-temporal sequence of cross-regulatory events in root meristem growth. *Proc. Natl. Acad. Sci. U S A.* 107(52):22734-9.
- 525 [27] Mitchison GJ, Hanke DE, Sheldrake AR. 1981 The polar transport of auxin and vein pattern in plants. *Phil. Trans. R. Soc. Lond. B* 7, 295, 1078, 461-471.

- [28] Miyawaki K, Matsumoto-Kitano M, Kakimoto T. 2004 Expression of cytokinin biosynthetic isopentenyltransferase genes in Arabidopsis: tissue specificity and regulation by auxin, cytokinin, and nitrate. *Plant J.* 37, 128-138.
- [29] Leyser HM, Pickett FB, Dharmasiri S, Estelle M. 1996 Mutations in the AXR3 gene of Arabidopsis result in altered auxin response including ectopic expression from the SAUR-AC1 promoter. *Plant J.* 10(3):403-13.
- [30] Rashotte AM, Carson SD, To JP, Kieber JJ. 2003 Expression profiling of cytokinin action in Arabidopsis. *Plant Physiol.* 132(4):1998-2011.
- [31] Takei K, Ueda N, Aoki K, Kuromori T, Hirayama T, Shinozaki K, Yamaya T, Sakakibara H. 2004 AtIPT3 is a key determinant of nitrate-dependent cytokinin biosynthesis in Arabidopsis. *Plant Cell Physiol.* 45(8):1053-62.
- [32] Band LR, Úbeda-Tomás S, Dyson RJ, Middleton AM, Hodgman TC, Owen MR, Jensen OE, Bennett MJ, King JR. (2012) Growth-induced hormone dilution can explain the dynamics of plant root cell elongation. *Proc. Natl. Acad. Sci. U. S. A.* 109(19):7577-82.
- [33] Fu X, Richards DE, Ait-Ali T, Hynes LW, Ougham H, Peng J, Harberd NP. 2002 Gibberellin-mediated proteasome-dependent degradation of the barley DELLA protein SLN1 repressor. *Plant Cell* 14(12):3191-200.
- [34] Rausenberger J, Tscheuschler A, Nordmeier W, Wüst F, Timmer J, Schäfer E, Fleck C, Hiltbrunner A. 2011 Photoconversion and nuclear trafficking cycles determine phytochrome A's response profile to far-red light. *Cell* 146(5):813-25.
- [35] Muraro D, Mellor N, Pound MP, Help H, Lucas M, Chopard J, Byrne HM, Godin C, Hodgman TC, King JR, et al. Integration of hormonal signaling networks and mobile microRNAs is required for vascular patterning in Arabidopsis roots. *Proc. Natl. Acad. Sci. U S A.* 2014 Jan 14;111(2):857-62.

- 555 [36] Laskowski M, Grieneisen VA, Hofhuis H, Hove CA, Hogeweg P, Marée AF, Scheres B. 2008 Root system architecture from coupling cell shape to auxin transport. *PLoS Biol.* 6(12):e307.
- [37] Birnbaum K, Shasha DE, Wang JY, Jung JW, Lambert GM, Galbraith DW, Benfey PN. 2013 A Gene Expression Map of the Arabidopsis Root.  
560 *Science* 302(5652):1956-60.
- [38] Scholl RL, May ST, Ware DH. 2000 Seed and molecular resources for Arabidopsis. *Plant Physiol.* 124(4):1477-80.
- [39] Pradal C, Dufour-Kowalski S, Boudon F, Fournier C, Godin C. 2008 OpenAlea: A visual programming and component-based software platform for  
565 plant modeling. *Funct. Plant Biol.* 35, 9 & 10 751-760.
- [40] Hiitola B. 2010 *Inkscape 0.48 Essentials for Web Designers book*. Packt Publishing. Birmingham, United Kingdom.